(*72*) Zimmerman, J. A.; Eyler, J. R.; Bach, S. B. H.; McElvany, S. W. 'Magic Number' Carbon Clusters: Ionization Potentials and Selective Reactivity. *J. Chem. Phys.* **1991**, *94*, 3556–3562.
(*73*) Ying, Z. C.; Jin, C.; Hettich, R. L.; Puretzky, A. A.; Haufler, R. E.; Compton, R. N. Production, Characterization of Metallofullerene 'Superatoms'. In *Recent Advances in the Chemistry and Physics of Fullerenes and Related Materials*; Kadish, K. M., Ruoff, R. S., Eds.; Electrochemical Society: Pennington, N.J., 1994, pp 1402–1412.
(*74*) Hettich, R. L.; Ying, Z. C.; Compton, R. N. Structural Determination and Ionic Properties of Endohedral Lanthanum Fullerenes. In *Recent Advances in the Chemistry and Physics of Fullerenes and Related Materials*; Kadish, K. M., Ruoff, R. S., Eds.; Electrochemical Society: Pennington, N.J, 1995, pp 1457–1464.
(*75*) Broclawik, E.; Eilmes, A. Density Functional Study of Endohedral Complexes M@C_{60} (M = Li, Na, K, Be, Mg, Ca, La, B, Al): Electronic Properties, Ionization Potentials, and Electron Affinities. *J. Chem. Phys.* **1998**, *108*, 3498–3503.
(*76*) Boltalina, O. V.; Ioffe, I. N.; Sorokin, I. D.; Sidorov, L. N. Electron Affinity of Some Endohedral Lanthanide Fullerenes. *J. Phys. Chem. A* **1997**, *101*, 9561–9563.
(*77*) Boltalina, O. V.; Dashkova, E. V.; Sidorov, L. N. Gibbs Energies of Gas-phase Electron Transfer Reactions Involving the Larger Fullerene Anions. *Chem. Phys. Lett.* **1996**, *256*, 253–260.
(*78*) Boltalina, O. V.; Markov, V. Y.; Lukonin, A. Y.; Avakjan, T. V.; Ponomarev, D. B.; Sorokin, I. D.; Sidorov, L. N. Mass Spectrometric Measurements of the Equilibrium Constants of Ion–Molecular Reactions of Fullerenes, Fluorine Derivatives and Endohedrals. In *Recent Advances in the Chemistry and Physics of Fullerenes and Related Materials*; Kadish, K. M., Ruoff, R. S., Eds.; Electrochemical Society: Pennington, N.J., 1995, pp 1395–1408.
(*79*) Hettich, R.; Lahamer, A.; Zhou, L.; Compton, R. Investigation of the Fragmentation and Oxygen Reactivity of Endohedral Metallofullerenes M@C_{60}. *Int. J. Mass Spectrom.* **1999**, *182/183*, 335–348.
(*80*) McElvany, S. W.; Holliman, C. L. Gas-phase Oxidation of Fullerene, Metallofullerene Ions. In *Recent Advances in the Chemistry and Physics of Fullerenes and Related Materials*; Kadish, K. M., Ruoff, R. S., Eds.; Electrochemical Society: Pennington, N.J., 1997, pp 772–782.

D. E. Giblin and M. L. Gross
Washington University, St Louis, Missouri, USA

Cluster Anions (Experiments)

Negative ions and excess electron states play many important roles in chemistry and related fields. Solvated anions govern a host of phenomena in solution. Solvated electrons are fundamental species in radiation chemistry. Electron defect states are the basis for a variety of electronic and optical phenomena in materials. All of these involve the interaction of negative ions or excess electrons with other atoms or molecules in their environments, and all of them have finite size analogues among cluster anions of appropriate size and composition.

A cluster anion is composed of two or more atomic or molecular components and an extra electron. A cluster anion can be classified in terms of the number of its components that are chiefly responsible for binding the extra electron (see Fig. 1). At one end of this classification scale, the extra electron is bound by a single component of the cluster forming a distinct sub-ion. Such cases are exemplified by solvated anion clusters, where a sub-anion interacts with the other neutral (solvent) components of the cluster. At the other end of this scale, the extra electron is bound by all of the components of the cluster, i.e., it is shared by essentially all of them. These are best exemplified by metal cluster anions made up of atoms from free electron metals. There, the extra electron "dissolves" in a sea of delocalized valence electrons provided by the component metal atoms of the cluster to become delocalized itself.

Between the extreme ends of this scale, the extra electron is bound by its interaction with an intermediate number of cluster components, i.e., by more than one, but by less than all. Cluster anions in this category require several (>1) components to form viable anionic species. Below their minimum size, such cluster anions either cease to form or lack kinship with their corresponding condensed phase phenomenon. Above their minimum size, the excess electron may remain relatively localized or become somewhat delocalized, depending on the particular species. Examples of such cases are found among cluster anion analogues to solvated electrons and color centers, both of which are electron defect phenomena in condensed phases. In solvated electron systems, the excess electron is bound by its collective interaction with several polar solvent molecules, and in such systems, the electron is often envisioned as residing in a "cavity" of oriented polar molecules. In color centers, an electron substitutes for a missing anion at an ionic lattice site and thus is bound largely by its shared interaction with nearby cations.

Another example of viable species in this category is temporary anions that require some minimum number of solvents to stabilize them. Excess electrons in nonpolar solvents may provide yet more examples,

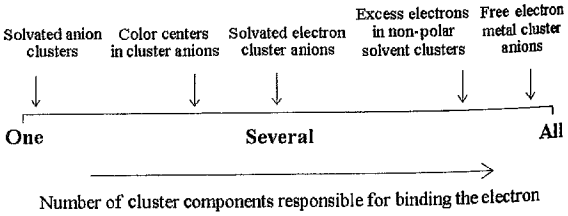

Figure 1
Scale for classifying cluster anions, illustrated with selected examples.

but if so, they probably sit at the border of the "charge shared by all" category. In bulk solvents of this type, the excess electron goes into the conduction band, where it shows no particular preference for one component over another. Thus, although a minimum number of atoms is probably required to form a cluster anion such as Xe_n^-, once the cluster is formed, it is also likely to be characterized by substantial excess electron delocalization. Nevertheless, from the examples given, it is clear that the sliding scale classification scheme put forth here is not entirely synonymous with a scale having localized charge species at one end and delocalized charge species at the other. Cluster anions are too diverse to be so easily classified, and even the scheme put forth here falls short of being a universal classification.

In what follows, we first review the available ion sources used to generate free (gas-phase) cluster anions and the experimental methods employed to study them. We then present brief summaries of selected experimental studies involving cluster anions. These are organized by technique but grouped according to whether the excess negative charge of the cluster anion is bound by *one*, by *several*, or by *all* of their atomic and/or molecular components. Together, these summaries provide a glimpse into how the study of cluster anions contributes to a molecular-level description of short-range interactions in condensed phase phenomena.

1. Sources of Cluster Anions

An impressive array of chemically diverse cluster anions can be formed with available sources, these making use of several different physical processes. Homogeneous and heterogeneous cluster anions of both molecular and metallic systems can be formed, with nearly every combination possible, in principle. Some of the sources that can generate cluster anions include; ion sputter (*1*), flow tube (*2*, *3*), Penning discharge (*4*), and high-pressure mass spectrometry (*5*, *6*) ion sources. Charged particle production methods used in these sources include electron beam bombardment (*7*), electrical discharges (*4*), proton beam irradiation (*8*), cesium or xenon ion beam sputtering, radioactivity (*9*), and the photoemission of electrons (*10*). Supersonic expansion sources for neutral species have often been married to ionization techniques to prepare beams of cluster anions. Using such neutral/ion hybrid sources, beams of cluster ions have been produced from supersonic expansion ion sources using corona discharges (*11*), radioactivity (*12*), and the photoemission of electrons (*13*) in the stagnation chamber behind the nozzle. Cluster anions have also been generated by injecting electrons (either by thermionic emission (*14*) or via beams of electrons (*15*)) directly into the expansion jet just beyond the nozzle orifice on its high vacuum side. Preexisting beams of neutral clusters, i.e., those well beyond the nozzle in the free molecular flow region of the expansion, have also been brought into contact with excited Rydberg states to form cluster anions (*16*). Other important hybrid sources employing supersonic expansions to generate cluster anions include laser vaporization sources (*17*), pulsed arc discharge sources (*18*), and electrospray sources (*19*). Hybrids of different inert gas condensation sources produce nanocluster anions either by injecting slow electrons directly into the exiting flow (*20*), or by forming anions inside the inert gas condensation source itself (*21*).

2. Experimental Methods Used to Study Cluster Anions

Information about cluster anions has been obtained through a variety of experimental approaches, including thermochemical measurements, photodestruction studies, threshold (tunable wavelength) photodetachment spectroscopy, photodissociation spectroscopy, fixed-frequency photoelectron spectroscopy, anion-ZEKE spectroscopy, infrared predissociation spectroscopy, collisional charge transfer experiments, and reactivity studies. Necessarily, the accuracies of the quantities measured with these techniques vary greatly, with thermochemical techniques providing the least and anion-ZEKE supplying the most accurate measurements.

Thermochemical measurements (*22*, *23*) were the earliest substantial sources of energetic information about solvated cluster anions, and together with negative ion photoelectron spectroscopy, they thus far have supplied the lion's share of energetic information about solvated cluster anions. Thermochemical data have been obtained from high-pressure mass spectrometry (see *Thermochemistry (Methods): Ion–Molecule Equilibria at High Pressure*), flow tube measurements (see *Instrumentation: Flow Tubes*), ion cyclotron resonance spectrometry (see *Instrumentation: Fourier Transform Ion Cyclotron Resonance*), and tandem mass spectrometry, with high-pressure mass spectrometry providing the majority of such results. Gas-phase thermochemical experiments on anion solvation provide equilibrium constants as a function of temperature for cluster anion association reactions of the type (Eqn. (1)),

$$A^-(B)_n + B \Leftrightarrow A^-(B)_{n+1} \qquad (1)$$

where A^- denotes the sub-ion within a cluster anion such as $A^-(B)_n$, B is a solvent molecule, and subscripts n and $n+1$ are solvation numbers. From these data, values of enthalpy and entropy changes, $\Delta H_{n,n+1}$ and $\Delta S_{n,n+1}$, are derived from van't Hoff plots. Sequential solvation energies are often obtained by assuming that $-\Delta H_{n,n+1} = D_0[A^-(B)_n \cdots B]$,

where the latter is the dissociation energy for $A^-(B)_{n+1}$ dissociating into $A^-(B)_n$ and B.

Photodestruction (*24*) and threshold photodetachment (*25*, *26*, *27*) spectroscopy (see *Thermochemistry (Methods): Photoelectron Spectroscopy of Negative Ion Beams: Measurements of Electron Affinities*) were among the earliest spectroscopic methods applied to cluster anions. In the former, a tunable beam of light interacts with a mass-selected beam of cluster ions, and the loss of those ions is measured as a function of photon frequency. This method, however, does not distinguish between loss resulting from electron photodetachment and that from photodissociation. In threshold photodetachment spectroscopy, electrons are photodetached from a mass-selected cluster anion beam by photons from a frequency-tunable source, and the signal is monitored as a function of photon energy.

In photodissociation spectroscopy (see *Ion Spectroscopy: Photodissociation Spectroscopy*) one typically pumps to an excited electronic state of the ionic complex and monitors ionic fragments as a function of photon energy (*28*, *29*). Many cluster anions do not exhibit low-lying electronically excited states accessible with visible (or nearly visible) photons. Typically, those that do are of two types: (i) complexes in which either the sub-ion or its neutral solvent(s) possess such states, which can then act as chromophores; and (ii) systems in which low-lying excited states arise because of complexation, i.e., as a result of anion–neutral interactions.

Anion photoelectron spectroscopy (see *Thermochemistry (Methods): Photoelectron Spectroscopy of Negative Ion Beams: Measurements of Electron Affinities*) is conducted by crossing a mass-selected beam of cluster anions with a fixed-frequency laser beam, and energy-analyzing the resulting photodetached electrons (*14*, *30*, *31*). This technique is governed by the energy conservation relationship, $h\nu = T + KE_{e^-}$, where $h\nu$ is the fixed-frequency photon energy, T is the transition energy from the initial negative ion state to the final neutral state (also referred to as EBE, the electron binding energy), and KE_{e^-} is the measured kinetic energy of the photodetached electron. This technique provides energetic information about cluster anions, including sequential solvation energies. Also, although this technique is conducted on cluster anions, it provides size- and composition-selected spectroscopic information about their corresponding neutral clusters as well.

In anion-ZEKE spectroscopy (see *Ion Spectroscopy: Photoelectron Spectroscopy, Threshold Photoelectron Spectroscopy, and Pulsed Field Ionization*), electrons are photodetached with nearly zero electron kinetic energy from mass-selected anions using a tunable laser (*32*). The resulting very low energy electrons are detected as a function of photon energy. Anion-ZEKE provides much higher spectroscopic resolution than does conventional anion photoelectron spectroscopy. Also, the threshold laws are different, making ZEKE peaks directly observable and easy to identify.

Infrared predissociation spectroscopy (see *Ion Spectroscopy: Vibrational Predissociation*) is most often conducted by intersecting a mass-selected beam of argon-solvated, cluster anions with a tunable-frequency infrared photon beam, and monitoring, as a function of photon energy, the intensity of those charged species that reflect the loss of argon (*33*). Because the argon is very weakly bound to the rest of the cluster anion, absorption of infrared photons causes the evaporation of one or more argon atoms, thereby signaling an absorption of infrared radiation at that frequency. Shifts in absorption frequencies lead to inferences about bond connectivity and thus about the structures of cluster anions.

Information on cluster anions has also been provided by collisional charge transfer experiments. At least two variants of this technique have seen use. In one, a velocity-variable beam of fast alkali metal atoms is crossed with a beam of neutral clusters while the formation of cluster anions is monitored mass spectrometrically as a function of collision energy (*34*). The observed chemi-ionization threshold energies are then used to determine electron affinities for small clusters. In the other, better-developed method, a neutral cluster beam is crossed with a beam of electronically excited Rydberg atoms (*35*). At their intersection point, charge transfer takes place, cluster anions are formed, and their intensities are monitored mass spectrometrically as a function of Rydberg principal quantum number. This latter technique has the advantage of providing a particularly well-characterized cluster anion formation environment.

Experiments using flow tubes and fast flow reactors (see *Instrumentation: Flow Tubes*) provide most of the available information about reactions between cluster anions and neutral molecules (*36*). These methods provide thermally controlled reaction environments for reactants for relatively long periods of time. Measurements of ionic product formation are typically conducted mass spectrometrically. Rate constants as a function of cluster size have been provided for a variety of reactions of atmospheric importance.

3. *Solvated Anions: Cluster Anions in which One Component Binds the Charge*

Around the end of the nineteenth century when physical chemistry was emerging as a distinct branch of chemistry, two topics were especially in fashion, colloids and electrolytes. The study of colloids focused on aggregation phenomena, whereas the study of electrolytes dealt with ions in solution. At the time, these two topics were viewed as being separate, and their paths were largely divergent. Interestingly, as new methods developed over the

intervening years, these two schools converged in modern times with the study of gas-phase solvated ions. Such species are cluster ions in which a core ion interacts with, i.e., is solvated by, one or more neutral molecules. Such ion–molecule complexes are governed by many of the same interactions that are at work in ion solvation in solution, and as such, their study offers a unique opportunity to gain insight into ion solvation at the microscopic level. As in many studies of cluster ions, an important degree of control is gained by the ability to select cluster species of the desired sizes and compositions and to interrogate their evolving properties as a function of their extent of solvation (*37*). Selected examples of anion solvation studies in the gas phase follow.

3.1 *Thermochemical Determinations of Anion–Neutral Interaction Energies*

Several groups have contributed to the store of data built-up by this technique, most notably those of Kebarle and Castleman. Figure 2 shows the enthalpy changes for the stepwise hydration (solvation with H_2O) of several negative ions in such thermochemical experiments (*38*). They clearly decrease with increasing cluster size. Analogous experiments with positive ions showed the same qualitative trend (see *Solvation and Clusters: Metal Ion Solvation*). Moreover, the results suggest that positive ion stepwise solvation energies converge to estimated bulk values at about five solvent molecules per cation. Anions, on the other hand, showed a significantly slower convergence to bulk, possibly because of their larger radii and greater perturbations on their neighboring solvent molecules.

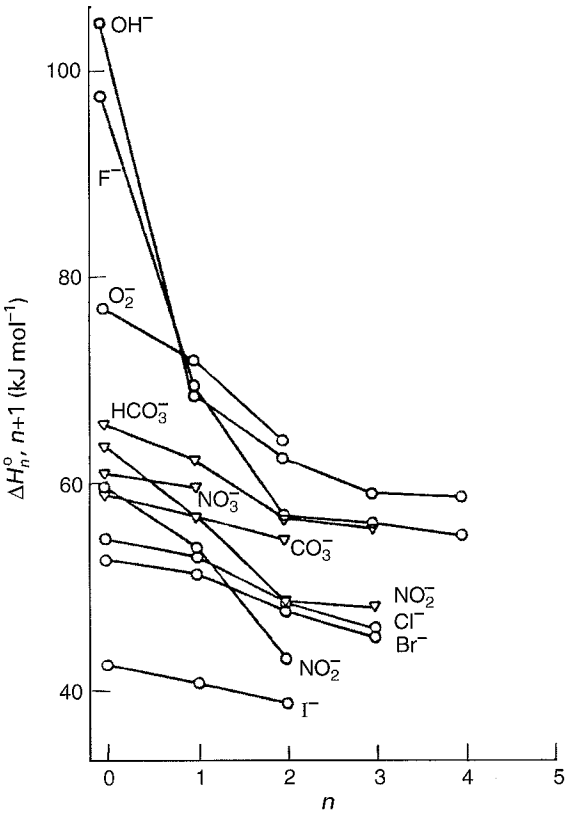

Figure 2
Enthalpy changes for the stepwise gas-phase hydration of several negative ions. (Adapted from *J. Chem. Phys.* **1980**, *72*, 1089–1094 (*38*).)

3.2 *Photoelectron Spectroscopy of Solvated Anions*

Among the earliest cluster anion systems to be studied by photoelectron spectroscopy was the NO^- anion solvated by N_2O molecules. In these studies (*14*), the spectra of $NO^-(N_2O)_n$ exhibit structured spectral patterns that strongly resemble those of free NO^-, but which are shifted with increasing size, n, to successively higher electron binding energies (see Fig. 3). This clearly demonstrates that the largely intact sub-ion, NO^-, acts as the chromophore for photodetachment, and that it is being solvated and stabilized by N_2O molecule(s). In addition to $NO^-(N_2O)_n$, numerous other $NO^-(\text{solvent})_n$ cluster anions have also been studied by photoelectron spectroscopy, including those in which the solvent was H_2O, NH_3, H_2S, Ar, Kr, Xe, and ethylene glycol (*39*). A major goal in making these measurements was the elucidation of ion–neutral interaction energetics.

Stepwise stabilization energies were one of the goals of photoelectron studies of the microsolvation of bithiophene and azulene anions by water (*40*) and of O_2^- and NO^- by aromatic molecules (*41*). Several other studies have focused on obtaining spectroscopic information about solvation shells. Results from studies of $I^-(N_2O)_n$, $I^-(CO_2)_n$, and $Br^-(CO_2)_n$ suggest first solvation shells containing eleven, nine, and eight solvent molecules, respectively (*42*). Work on $NO_3^-(H_2O)_n$ found that the first solvation shell around NO_3^- contains only three water molecules (*43*). In an investigation of $O^-(Ar)_n$, the first solvation shell was found to close at $n = 12$, with a strongly implied icosahedral structure (*44*). Examination of the $(n+1)^{-1/3}$ dependence of the electron affinity data ($n > 12$) showed that it extrapolated to the expected value for an O^- impurity in an argon matrix.

3.3 *Anion-ZEKE Spectroscopy of Solvated Anions*

High resolution anion-ZEKE spectroscopy has been applied to the study of simple solvated anions by

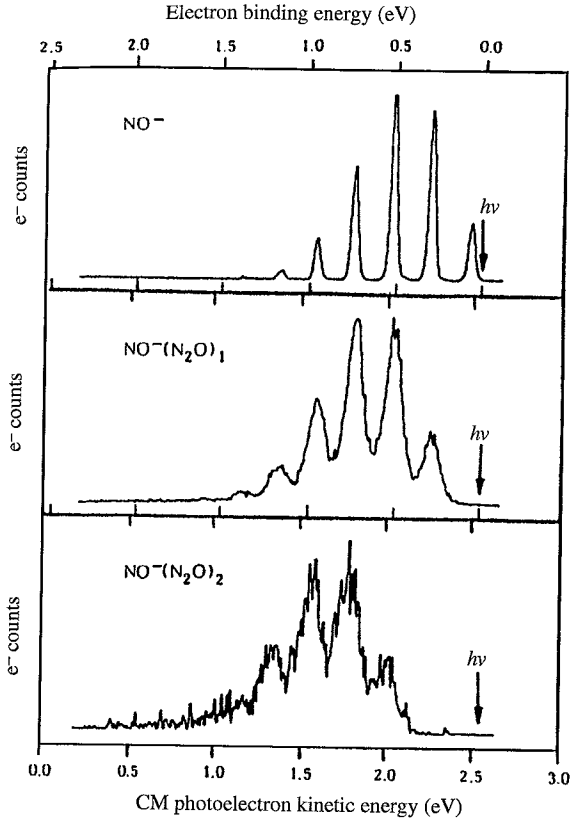

Figure 3
Anion photoelectron spectra of NO^-, $NO^-(N_2O)_1$, and $NO^-(N_2O)_2$ showing that the sub-ion, NO^-, acts as the chromophore in both cluster anions. (Reproduced by permission of the American Institute of Physics from *J. Chem. Phys.* **1987**, *87*, 4302–4309 (*39*).)

several investigators. The anion-ZEKE technique is akin to the neutral ZEKE method originally developed by Müller-Dethlefs and Schlag (*45*). Examples of cluster anions studied include $I^-(H_2O)$, $I^-(Xe)_n$, $Cl^-(Ar)_n$, $I^-(CO_2)$, and $I^-(CH_3I)$. These spectra tend to reveal the low-frequency vibrational structure resulting from excitation of van der Waals modes in the cluster anion's corresponding neutral, and together with information from anion photoelectron spectroscopy on high-frequency modes, they permit the construction of detailed anion and neutral potential energy curves.

3.4 Photodissociation Studies of Solvent Caging in Solvated Anion Complexes

A study of particular relevance to ion solvation involved the photodissociation of $Br_2^-(CO_2)_n$ and

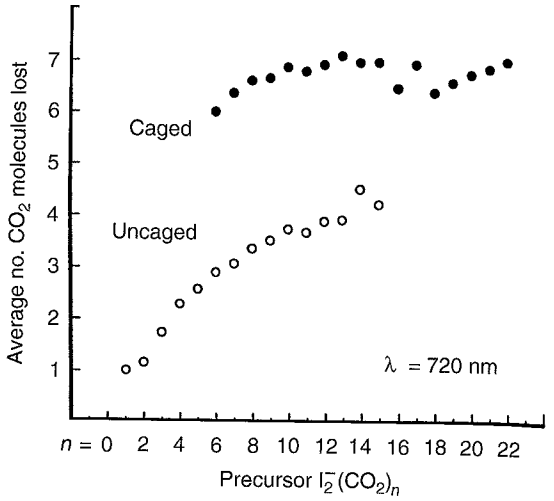

Figure 4
Average number of CO_2 molecules lost to form caged and uncaged photofragment ions following the absorption of a 720 nm photon by $I_2^-(CO_2)_n$ precursors. (Reproduced by permission of the American Chemical Society from *J. Phys. Chem.* **1991**, *95*, 8028–8040 (*46*).)

$I_2^-(CO_2)_n$. In these experiments, the Br_2^- and I_2^- moieties were photoexcited above their dissociation limits and the quantum yields for the two processes (Eqns. (2) and (3))

$$X_2^-(CO_2)_n + h\nu \rightarrow X^-(CO_2)_m + (n-m)CO_2 + X \quad \text{uncaged} \qquad (2)$$

$$X_2^-(CO_2)_n + h\nu \rightarrow X_2^-(CO_2)_p + (n-p)CO_2 \quad \text{caged} \qquad (3)$$

were measured as a function of n (*46*). A strong increase in caging efficiency occurred around $n = 12$, when $X = Br$ and around $n = 16$, when $X = I$, with complete caging thereafter in both systems. The onset of complete caging was interpreted in terms of the X_2^- core being surrounded by a complete solvent shell of CO_2 molecules (see Fig. 4). Subsequent ultra-fast spectroscopic studies probed the dynamics of this and related systems. The photodissociation dynamics of $I_2^-(CO_2)_n$ were studied by anion femtosecond photoelectron spectroscopy. The time scales for a variety of caged and uncaged processes were determined (*47*). In addition, femtosecond stimulated emission pumping in coordination with femtosecond photoelectron spectroscopy was used to monitor the dynamics within $I_2^-(CO_2)_n$ following vibrational excitation of the I_2^- chromophore (*48*).

3.5 Competition Between Photodetachment and Photodissociation

In some anionic clusters, e.g., $I^-(CH_3X)$, both photodissociation and photodetachment compete. Studies of $I^-(CH_3X)$, which is an intermediate in the S_N2 reaction of $I^- + CH_3X$, enabled an examination of both of these channels (*49*). From the combined results, it was concluded that charge-transfer excited states in $I^-(CH_3X)$ lie near the detachment continuum of the anion complex. Furthermore, vibrational structure observed in the photoelectron portion of the experiment implied that the C–X bond in the CH_3X component of the complex was elongated, as predicted by theory. The above mentioned anion-ZEKE technique has also been brought to bear on this system (*32*).

3.6 Dissociation Dynamics of the Neutral Products of Cluster Anion Photodetachment

When electrons are photodetached from cluster anions, the resulting neutral products often contain enough excess energy to undergo dissociation. Continetti and co-workers (*50*) have developed a photoelectron–photofragment coincidence spectroscopic technique for exploring the dissociative photodetachment dynamics of the neutral cluster product species following photodetachment of its corresponding cluster anion. This technique has been applied to the study of numerous solvated cluster anions. In the cases of $O^-(H_2O)_2$ and $OH^-(H_2O)_2$, for example, the three body dissociation dynamics of the neutral photodetachment products were investigated by measuring recoil angles and velocities of each fragment in coincidence. From the observed partitioning of momentum, either a two-step mechanism or dissociation from a wide variety of initial geometries was implicated.

3.7 Vibrational Predissociation Spectra of Solvated Anions

Vibrational predissociation spectroscopic studies have been conducted on a number of solvated anions, examples being $I^-(H_2O)$, $I^-(HDO)$, $I^-(H_2O)Ar$, $Cl^-(H_2O)$ and $I^-(H_2O)N_2$ (*51–53*). In all cases, these experiments reveal the couplings of motions and thus the gross geometric structure of such complexes. In an extensive set of vibrational predissociation experiments, the structure of $X^-(H_2O)_n$ cluster anions was solved (X^- is a halogen atomic anion). With the exception of $F^-(H_2O)_n$, where F^- is centro-symmetrically (internally) solvated, the other halogen atomic anions sit on the outside of the water moiety (external). This, of course, is at odds with the traditional picture of ion solvation. In other vibrational predissociation experiments, it was shown that four water molecules are required to complete the coordination shell around O_2^- in $O_2^-(H_2O)_n$ and that the water molecule in $SO_2^-(H_2O)_1$ exhibits a symmetrical binding structure, with each hydrogen atom binding to an oxygen atom in SO_2^-.

3.8 Electronic Absorption Spectra of Solvated Anions

Johnson *et al.* have explored the absorption spectra of size-selected $I^-(H_2O)_n$ cluster anions by taking the action spectra of their photoexcited complexes (*54*). They found that the absorption spectra of $I^-(H_2O)_n$ cluster anions began to evolve toward the charge-transfer-to-solvent (CTTS) band of I^-_{aq} even at small cluster anion sizes.

3.9 Reactivity Studies with Solvated Anions

Fast flow reactors (*55*) have supplied a treasure trove of information about the kinetics and mechanisms of hydrated anion reactions operating under well-defined conditions of temperature and pressure. For example, $OH(H_2O)_{0-1}$ was found to react with acetonitrile at near collision rates by way of proton transfer and ligand switching mechanisms. Interestingly, however, further hydration greatly reduces its reactivity, probably because of the thermodynamic instability of the products relative to the reactants. In another example, the case of $OH^-(H_2O)_n$ reacting with SO_2, its mechanism was found to proceed mainly via ligand switching (*56*). Figure 5 shows the dependence of rate constants on cluster size for reactions of $OH^-(H_2O)_n$ with SO_2 at 135 K. In

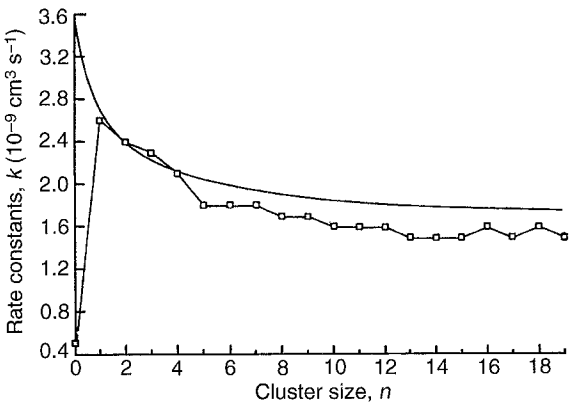

Figure 5
Dependence of rate constants on cluster size for the reactions of $OH^-(H_2O)_n$ with SO_2 at T = 135 K. The open boxes indicate experimental points, and the solid line shows calculated results. (Reproduced by permission of the American Chemical Society from *J. Phys. Chem.* **1991**, *95*, 6182–6186 (*56*).)

addition to homogeneous gas phase reactivity studies, heterogeneous reactions have also been investigated. An example is the determination of the cluster size dependence of charge transfer from $I_2^-(CO_2)_n$ cluster anions during their collisions with silicon surfaces (*57*).

4. *Cluster Anions in which Several Components are Required to Bind the Charge*

Here, we present examples of studies that focused on cluster anions in which more than one (but less than all) of their components are needed to bind the excess negative charge. Many of these are cluster anion analogues to condensed phase phenomena that do not have stable atomic or molecular counterparts. These cluster anions, by definition, require a minimum number of components to form. By way of comparison, solvated anions with distinct charge-localized sub-ions do have atomic or molecular counterparts in the sense that the sequential removal of all of their solvents would still leave the sub-ion as its core phenomena. On the other hand, removal of one more molecule from an ammoniated electron (solvated electron) cluster anion containing 34 ammonia molecules would cause the resulting cluster anion to become unstable. Likewise, the removal of one more water molecule from a hydrated pyridine anion containing three water molecules causes this system to disappear. There are many examples. Analogues to color centers in alkali halide cluster anion cuboids cease to exist below a critical size of 13 molecules. Hydrated amino acid anions do not sustain themselves as zwitterions with fewer than five water molecules. There are also examples where a recognizable condensed phase property disappears below some critical cluster size even though the resulting smaller size cluster anions may remain stable. An example of this is the loss of metallic behavior in magnesium cluster anions below 18 magnesium atoms per cluster. Clearly, below some number of cooperatively interacting cluster components, "the bubble bursts", and the condensed phase phenomena or property of interest ceases to exhibit a finite size, cluster analogue. Cluster anions are a particularly useful vehicle for studying condensed phase phenomena that depend on some threshold number of atoms or molecules. Among the techniques that have contributed to the study of these systems are mass spectrometry, anion photoelectron spectroscopy, electronic and vibrational (action) spectroscopies, and Rydberg electron transfer spectroscopy.

4.1 *Mass Spectrometric Studies*

Almost all of the cluster anions in this category were initially found via mass spectrometry. The existence of water cluster anions $(H_2O)_n^-$, starts with $n=2$ and ammonia cluster anions $(NH_3)_n^-$, begins at $n=34$ (*58*). The threshold size of hydrated pyridine cluster anions contains three water molecules. The smallest stable carbon dioxide cluster anion is its dimer (*59*). The phenol dimer anion is its smallest viable cluster anion size. The doubly-charged anion, $SO_4^{=}$, requires three water molecules to stabilize it (*60*). The smallest viable magnesium cluster anion is its trimer (*61*). The smallest stable benzene cluster anion begins at size, $n = 53$ (*62*).

4.2 *Anion Photoelectron Spectroscopy*

Negative ion photoelectron spectroscopy has been utilized to study solvated electron cluster anions, dipole-bound anions, solvent-stabilized anions, multiply-charged anion clusters, and color center cluster anions. Here, we summarize some of the highlights of these studies. The study of solvated electron clusters has been a particularly rich field of study. Work in this area was initially motivated by the observation that although individual water molecules do not bind excess electrons, bulk water readily solvates them, implying that the association of electrons with water is a multibodied interaction requiring a collection of molecules. After mass spectrometric work (*58*) showed that water cluster anions form at $n=2$, 6, 7, and from 11 on up in size (with much weaker intensities of $n=3$, 5, 8–10 also present), the anion photoelectron spectra of $(H_2O)_n^-$ was measured for the sizes, $n=2$, 3, 6, 7, 11–69.

The plot of their vertical detachment energies, VDE, vs. $n^{-1/3}$ (1/radius) suggested that, from $n=11$ on up in size, they bore a kinship to hydrated electrons, at least in many respects (*63*). Contributions were also made to the study of the 'missing' (weak intensity) cluster sizes (*64*). In addition, the photoelectron spectra of $(NH_3)_n^-$ for the sizes $n=41$–1,100 have been measured (*65*). In this case (see below), the plot of VDE vs. $n^{-1/3}$ (see Fig. 6) suggests that all of these cluster anion sizes exhibit a kinship with bulk ammoniated electrons. (At $n=1{,}100$, these cluster anions are ~4.8 A in diameter.) In addition to anion photoelectron experiments on homogeneous cluster anion systems, studies on $[Na_m(NH_3)_n]^-$ have been carried out in order to explore how sodium and its clusters are solvated (and ionized) in small ammonia clusters (*66*). (Dropping metallic sodium into liquid ammonia forms ammoniated electrons.)

Furthermore, femtosecond photoelectron studies on $I^-(D_2O)_n$ and $I^-(NH_3)_n$, have been conducted (*67*). Both cluster anion systems exhibit broad charge-transfer-to-solvent (CTTS) absorption bands analogous to those seen in their corresponding I^- solutions. Excitation of these bands in bulk solution leads to electron ejection from I^- and ultimately to the formation of their corresponding solvated

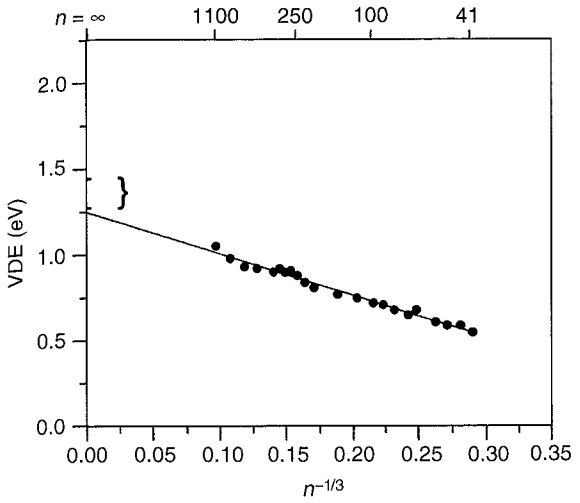

Figure 6
Plot of vertical detachment energy, VDE(n) vs. $n^{-1/3}$ for $(NH_3)_n^-$, $n = 41$–1,100. The VDEs show a linear dependence with $n^{-1/3}$ ($\sim$1/radius). The range of experimentally reported photoemission threshold energies for the bulk ammoniated electron is indicated by a bracket along the ordinate. (Reproduced by permission of the American Institute of Physics from *J. Chem. Phys.* **2002**, *116*, 5731–5737 (*65*).)

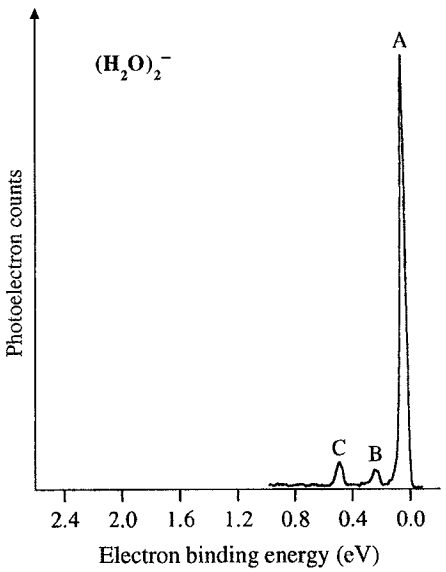

Figure 7
Anion photoelectron spectrum of ground-state, dipole-bound $(H_2O)_2^-$, illustrating the distinctive spectral signature of dipole-bound anions in photoelectron spectroscopy. (Reproduced by permission of Plenum Publishers from Naaman, R., Vager, Z., Eds. *The Structure of Small Molecules and Ions;* 1988 (*68*).)

electrons. Femtosecond photoelectron studies were performed to explore the solvent dependence of excess electron solvation dynamics in these species. These experiments were conducted by initially exciting the electron with an ultra-fast pump pulse and then detaching it with a time-delayed ultra-fast probe pulse. The resulting photoelectron spectra were recorded as a function of delay time in order to follow the temporal evolution of the photoexcited state. Significant differences were found between these two systems. Whereas the $I^-(D_2O)_n$ system proceeded through an initially excited dipole-bound state (see below), the $I^-(NH_3)_n$ system displayed no evidence of a dipole-bound state and the onset of its electron solvation dynamics was more gradual than in the $I^-(D_2O)_n$ case.

When the dipole moment of a molecule or cluster is large enough ($\mu > 2.5$ D), it may trap an excess electron in its electrostatic field to form what is usually referred to as a dipole-bound anion (see *Theory (Energies and Potential Energy Surfaces): Anions*). Although some molecules can form dipole-bound anions themselves, here we focus on small, dipole-bound cluster anions in which the molecular sub-components alone are not capable of dipole binding. An example is $(H_2O)_2^-$. As mentioned above, an individual water molecule cannot bind an electron. Neither a normal valence anion nor a dipole-bound anion of H_2O^- is stable [$\mu(H_2O) = 1.8$ D]. However, when two water molecules combine to form a hydrogen bonded dimer, its composite dipole moment becomes >2.5 D, and the dipole-bound species $(H_2O)_2^-$ can form. Numerous dipole-bound anions have been studied by photoelectron spectroscopy, finding a distinctive spectral fingerprint (*68*). This signature, which consists of a narrow, intense peak at low electron binding energy and weaker peaks resulting from molecular vibrations at higher electron binding energies (see Fig. 7), allows for the identification of dipole binding in anions. With this tool in hand, one sees that some dipole-bound cluster anions and solvated electron clusters are closely related. Although this relationship is most clearly the case for several water cluster anions, which appear to be precursors to hydrated electron cluster anions, it has also been seen in the case of $(HF)_3^-$. Complementary experimental and theoretical studies (*69*) have found the $(HF)_3^-$ cluster anion to have two isomers, one of which is dipole bound, whereas the other involves a HF molecule on one side of the excess electron and a hydrogen fluoride dimer $(HF)_2$, on the other, i.e., solvation of the electron from two sides.

There are many anions that are unstable in isolation (temporary anions) but which are nevertheless stable in condensed phases. In solution, such anions are stabilized by their solvent environment. At the molecular level, the effect of solvation on anion

stability can be explored by forming solvent-stabilized cluster anions, thereby mimicking some of the main effects that are operative in condensed phases. (Some of these were mentioned in the mass spectrometry section above.) There have now been several anion photoelectron studies of solvent-stabilized anions. Studies of the stabilization of the anions of naphthalene, pyrimidine, styrene, and pyridine by water solvent molecules, find only one water to be necessary in order to bring the first three down in energy into stability, whereas three water molecules were required to stabilize the pyridine anion. Other studies also explored the solvent-stabilization of the naphthalene anion (*70*) and several other systems, including the pyridine anion solvated by carbon dioxide solvent molecules. These photoelectron studies provide sequential solvation energies for the successive addition of solvent molecules, and by extrapolation, these studies also determined the electron affinity of the unseen aromatic molecule itself. They were able to identify the charge carrier from the observed vibrational structure. In the case of naphthalene/water cluster anions, for example, the excess electron appears to be localized on naphthalene, seeming to place it in the first category where one component binds the charge. This puts it in a curious situation, however, because more than one component, i.e., one naphthalene and one water, are needed to make it a viable species, putting it in the second category where a minimum number greater than one is required. A similar situation occurs for homogeneous solvent-stabilization in benzene cluster anions. Benzene has a much more negative electron affinity value than the species mentioned above, and thus should be very difficult to solvent-stabilize. Nevertheless, it is found that 53 benzene molecules are needed to stabilize a benzene cluster anion. From its VDE vs. $n^{-1/3}$ plot, it was concluded that $(\text{benzene})_n^-$ clusters with $n > 53$ exist in a bulk-like electron solvated state.

Several of the most common negative ions in wet chemistry are multiply-charged anions. Yet, these ions are not stable in isolation. They, like the temporary anions discussed above, require solvation to stabilize them, and again, from a molecular perspective, the number of solvents required to form a viable multiply-charged anion is an important issue. Recently, Wang *et al.* (*60*) have made spectacular advances in this direction. Using an electrospray ion source coupled to an anion photoelectron spectrometer, $SO_4^{=}(H_2O)_n$ doubly-charged cluster anions were generated and their photoelectron spectra were obtained. These studies provide energetic information that, together with calculations, led to a better understanding of the hydrogen bonding between SO_4^{2-} and water.

Color centers (F-centers) in alkali halide salt crystals form when an electron substitutes for a halogen anion in a vacancy site. The smallest alkali halide cluster to possess such a vacancy is a $3 \times 3 \times 3$ cuboid having 27 sites, i.e. $(MX)_{13}^-$, where MX is an alkali halide. Some 26 of these sites are, of course, occupied by either alkali or halogen atoms, whereas the 27th site is vacant and available for the extra electron. Thus, the F-center phenomena observed in bulk alkali halide crystals depends on some minimum number of alkali halide molecules and an excess electron, and it is another example of a phenomenon that has no molecular counterpart. Negative ion photoelectron spectroscopy has been brought to bear in the study of both stoichiometric and alkali-rich, alkali halide cluster anions (*71*). As a result of these studies $(KI)_{13}^-$ was interpreted as being an F-center species having a $3 \times 3 \times 3$ cubic arrangement (with a single excess electron occupying the corner anion vacancy), whereas $(NaCl)_{22}^-$ was proposed to be a corner F-center species with a $3 \times 3 \times 5$ structure. For $K_{1,2}(KI)_{n \geq 13}^-$ and $Na(NaCl)_{n \geq 21}^-$, it was proposed that their multiple excess electrons could be localized, depending on the specific cluster anion size, either separately in different F-center sites, or together as spin pairs in M^- sites, analogous to bipolarons in bulk crystals. Also, for certain small, alkali-rich cluster anions, it was proposed that two excess electrons could be localized together in single anion vacancies as F′ centers. In addition, photoelectron spectra of gas-phase $(CsI)_n^-$ nanocrystals containing between 26 and 330 atoms were also measured. This work extended the size range up into the nanometer regime. Bulk correlations observed there provided evidence for the existence of both F and F′ embryonic color centers in large, negatively charged, cesium iodide nanocrystals.

4.3 Electronic Absorption (Action) Spectroscopy

Among the most prominent characteristics of the bulk hydrated electron is its electronic absorption spectrum, which peaks at ~ 1.7 eV. To explore how water cluster anions are related to bulk hydrated electrons, the absorption spectra of size-selected hydrated electron clusters $(H_2O)_n^-$, have been measured over the range, $n = 6$–50 (*72*). These spectra were acquired as photodestruction action spectra, i.e., the absorption of light as a function of wavelength resulted in the depletion of the particular cluster anion under study. At the smaller sizes, the absorption spectra measured in this way were intense, narrow, and strongly red-shifted relative to the bulk absorption spectrum of the hydrated electron. Nevertheless, they march smoothly with increasing cluster anion size toward the bulk absorption spectrum.

4.4 Vibrational Predissociation and IR Autodetachment Spectroscopy

In their seminal work, Johnson *et al.* (*33*) conducted vibrational predissociation studies of $(H_2O)_6^-Ar_n$

(see *Ion Spectroscopy: Vibrational Predissociation*). They utilized the fact that argon atoms are evaporated upon the absorption of infrared photons to map the vibrational spectrum of $(H_2O)_6^-$. The signal was collected by monitoring the photofragmentation of $(H_2O)_6^-Ar_n$ (see Fig. 8). Both strong and weak bands were observed. They assigned the strong ones to hydrogen atoms interacting with the excess electron and the weaker ones to a three-dimensional structure similar to that in the parent neutral cluster. Relatively small water cluster anions have also been studied in infrared autodetachment experiments. There, the data were acquired via the detection of both photofragmentation and photodetachment action spectra. Strong bands were observed in a frequency region indicative of single donor water vibrations in extended networks. These results, together with theoretical calculations, point to linear, "chain-like" $(H_2O)_n^-$ species.

4.5 *Reactivity of Hydrated Electron Clusters*

The reactions of water cluster anions over the size range, $n = 15$–30, have been examined with several neutral electron scavengers in a selected ion flow tube apparatus (see *Instrumentation: Flow Tubes*). Reactions with O_2, CO_2, and NO yielded mostly solvated charge transfer ions. The number of neutral water molecules lost during these reactions was strongly correlated to the reaction exothermicities (*73*).

4.6 *Rydberg Electron Transfer Spectroscopy*

Among the earliest systems in this category to be studied by Rydberg electron transfer (RET) were water cluster anions $(H_2O)_n^-$ (*74*). In addition, extensive studies of dipole-bound cluster anion formation and solvent stabilization of otherwise unstable valence anions have been carried out. Although they have also studied dipole-bound molecular anions, we here briefly summarize some of the work involving dipole-bound cluster anions in which the individual molecular sub-components alone are not capable of dipole binding, i.e., they require more than one component to bind their excess electrons. As in anion photoelectron spectroscopy, dipole binding in Rydberg electron transfer spectroscopy also displays a distinctive signature, seen as a sharp peak in the anion intensity vs. Rydberg quantum number spectrum. Among the many systems studied are dimer anion complexes made up of adenine(imidazole), adenine(pyrrole), adenine (water), pyrrole(water), and imidazole(water) combinations (see Fig. 9). In the work dealing with solvent stabilization of anions, stepwise solvation studies were utilized to estimate the values of negative electron affinities for a series of N-heterocyclic molecules and nucleic acid bases (*35*). The approach involved observing the size threshold for the formation

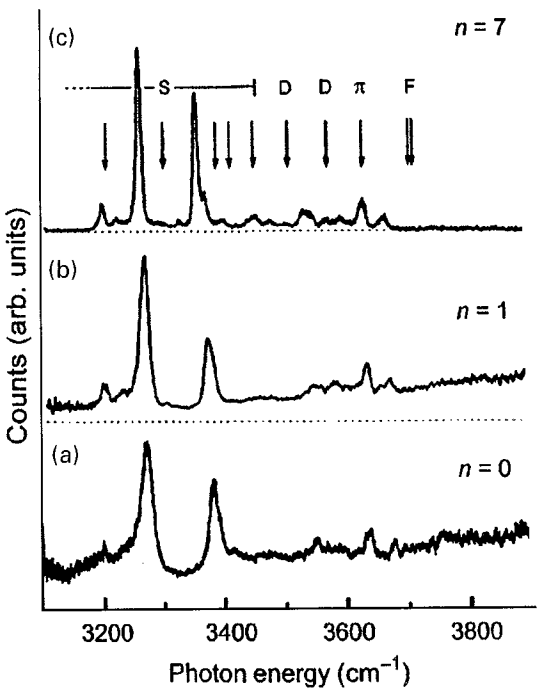

Figure 8
Infrared spectra of $(H_2O)_6^-Ar_n$ with $n = 0$, 1, and 7. (a) and (b) are the action spectra of $(H_2O)_6^-$ and $(H_2O)_6^-Ar$, respectively. The spectrum of $(H_2O)_6^-Ar_7$ (c) was detected via vibrational predissociation (decay to $(H_2O)_6^-$). (Reproduced by permission of the American Institute of Physics from *J. Chem. Phys.* **1998**, *108*, 444–449 (*33*).)

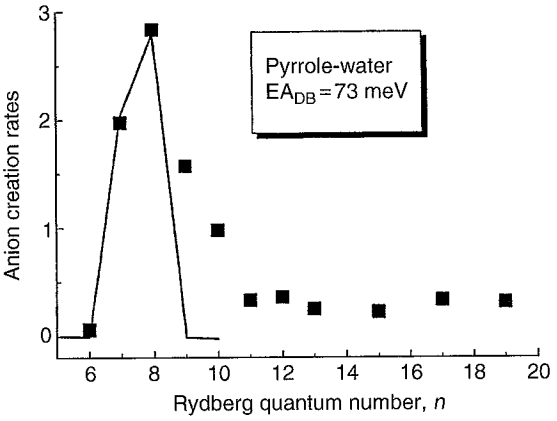

Figure 9
Rydberg electron transfer spectrum of the dipole-bound, pyrrole(water) dimer anion. EA_{DB} is the electron affinity of the dipole-bound species. (Reproduced by permission of the American Chemical Society from *J. Phys. Chem. A* **2000**, *104*, 10662–10668 (*35*).)

of solvent-stabilized valence anions and then using semiempirical intermolecular potentials to calculate the corresponding neutral and anionic solvation energies, from which electron affinities were derived.

5. *Cluster Anions in which All of the Components Bind the Charge*

The clearest examples of cluster anions in which all of the components are responsible for binding the excess electron are those made up of atoms from free electron metals (see *Solvation and Clusters: Metal Clusters*). The electronic structure of such atomic clusters can be described, in large part, by the shell model. In this electronic model, the motion of the valence and excess electrons is envisioned as being governed by the smeared-out positive potential of the cationic nuclei of the atoms. The result is a high degree of electronic delocalization and a sequence of electronic shell closings that differ from those in atomic physics and thus the periodic table (*75*). Included among free electron metals are the alkali metals, the noble metals, and aluminum. Other elements and their clusters may also be amenable to a shell model description to one extent or another, but this usually must be demonstrated empirically. Here, we will focus on selected studies involving Li_n^-, Na_n^-, K_n^-, Rb_n^-, Cs_n^-, Cu_n^-, Ag_n^-, Au_n^-, and Al_n^-.

Before surveying the studies done on these systems, however, we note that many other metal, semiconductor, and metal or semiconductor compound cluster anions do not fit neatly into the classification scheme we are using here. This is not to say that they could not, in principle, be classified in this way, but only that they often defy being placed along the scale in Fig. 1 because of the complexity of their electronic structure. Some examples of such cluster anions are Fe_n^-, Co_n^-, Re_n^-, Pt_n^-, Ni_n^-, Pd_n^-, C_n^-, Nb_n^-, Pb_n^-, Si_n^-, Ge_n^-, Sn_n^-, Bi_n^-, $In_nP_m^-$, $Ga_nP_m^-$, B_nN^-, Si_nH^-, V_n^-, $V_2C_2^-$, $Co_2C_2^-$, Hg_n^-, Ti_n^-, Cr_n^-, FeO_y^-, Al_4C^-, MnO_4^-, $Fe_nS_m^-$, $Co_nO_m^-$, Zn_n^-, Mn_n^-, KAl_{13}^-, Co_n^-/benzene anionic complexes, metcar (metal–carbon) anions, and fullerene anions (see *Solvation and Clusters: Covalent Clusters of Group 14 Elements*).

5.1 *Mass Spectrometric Studies*

Mass spectral studies on sodium cluster cations exhibited peaks and steps at cluster sizes corresponding to shell closing numbers, and those observations ignited interest in the shell model (see *Solvation and Clusters: Metal Clusters*). Among cluster anions made up of atoms from free electron metals, mass spectrometric studies have often supported the shell model. Aluminum cluster anions produced using laser vaporization sources exhibited magic number peaks in the resulting mass spectra at $n = 13$, 23, and 37 (*76*). Alkali cluster anions generated by injecting electrons into supersonic expansions of alkali metals and argon also exhibited shell model, magic numbers in their mass spectra, as did potassium cluster anions formed by Rydberg electron transfer. Even magnesium cluster anions show strong magic number behavior, even though it was not clear before the fact that they should do so.

5.2 *Anion Photoelectron Spectrometry*

Negative ion photoelectron spectroscopic experiments have been conducted on copper, silver, and gold cluster anions. Relatively small cluster anions can be formed in a flowing afterglow ion source. From their spectra, adiabatic electron affinities, vibrational frequencies, bond length changes (between anions and their corresponding neutrals), and dissociation energies can be determined (*77*). Using different source technology, photoelectron spectra for copper and gold cluster anions containing as many as 600 atoms per cluster can be obtained. These spectra reveal the evolution of the d-band toward the bulk (*78*). The photoelectron spectra of copper cluster anions have also been determined for the purpose of comparing the observed electronic level structure with the predictions of the shell model (*79*). Substantial agreement was found, if ellipsoidal distortions, shake-up processes, multiplet splittings, and s–p hybridization were taken into consideration. In addition, the photoelectron (and plasmon absorption) spectra of silver cluster anions, and the photoelectron spectra of small, mixed silver/gold cluster anions have been measured.

The photoelectron spectra of aluminum cluster anions have also been recorded. The 3s and 3p levels in atomic aluminum are widely separated, and the shell model should not start to become valid until the s-derived and p-derived "bands" overlap. Studies show that this closure occurs at $n = 9$, and signatures for shell closings were found at the following anion and neutral cluster sizes, Al_{11}^-, Al_{13}^-, Al_{19}^-, Al_{23}^-, Al_{35}^-, Al_{37}^-, Al_{46}, Al_{52}, Al_{55}^-, Al_{56}, Al_{66}, and Al_{73}^- (*80*). These stable clusters correspond well to predicted spherical shell closings and corresponding closed shell neutral and cluster anions of trivalent aluminum, as shown in Fig. 10.

The anion photoelectron spectra of Li_n^-, Na_n^-, K_n^-, Rb_n^-, Cs_n^- as well as several small mixed alkali cluster anion spectra have been measured. The study of potassium cluster anions, $K_{n=2-19}^-$, provided the first direct, quantitative confirmation of the presence of jellium-like electronic shell structure in metal cluster anions (*81*). These spectra are highly structured and provided not only electron affinities but also electronic splittings for each cluster size. A strong correlation was found between the predicted shell model energy levels and the observed patterns and spacings in the spectra.

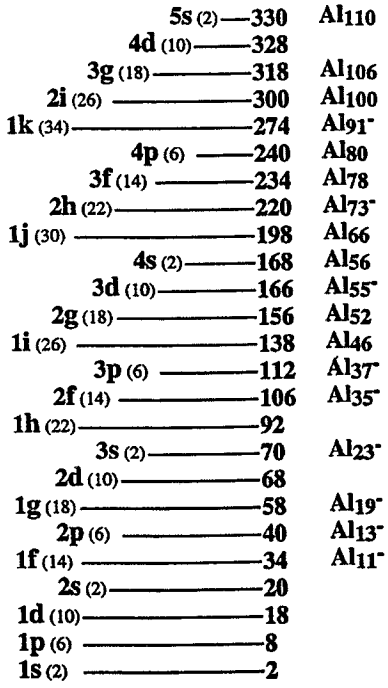

Figure 10
Spherical shell closings and corresponding closed-shell neutral and negative clusters of trivalent aluminum. The number in the parentheses after each shell index indicates the occupation number, $2(2l+1)$, of the shell, where l is the angular momentum quantum number. (Reproduced by permission of the American Physical Society from *Phys. Rev. Lett.* **1998**, *81*, 1909–1912 (*80*). Copyright (1998) by the American Physical Society.)

Because the mass spectral data show magnesium cluster anions to exhibit shell model behavior, they are also included in the present discussion. A collection of metal atoms does not necessarily exhibit metallic properties. The photoelectron spectrum of magnesium cluster anions was measured with the intention of watching the s-derived and the p-derived orbital "fans" converge (*61*). As shown in Fig. 11, at the cluster size where $\Delta = 0$, electrons from the lower occupied "fan" of orbitals spill into the previously unoccupied 3p-derived "fan", creating a partially filled band and meeting the criterion for the onset of metallic behavior. This condition was met at $n = 18$ in magnesium clusters.

5.3 *Collisional and Reactivity Studies*

A dramatic manifestation of shell model behavior was found while studying etching reactions of aluminum anion clusters with oxygen (*76*). Reactions of O_2 with Al_n^- were found to vary substantially with

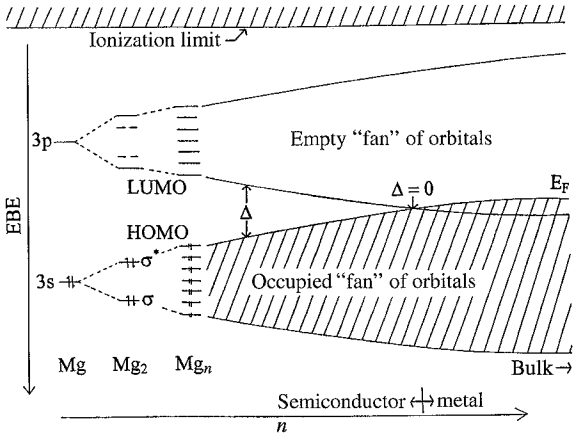

Figure 11
Schematic of the evolving electronic structure of magnesium. HOMO, LUMO, and EBE refer to the highest occupied molecular orbital, the lowest unoccupied molecular orbital, and the electron binding energy, respectively. (Reproduced by permission of the American Physical Society from *Phys. Rev. Lett.* **2002**, *89*, 213403/1–213403/4 (*61*). Copyright (2002) by the American Physical Society.)

cluster size, with Al_{13}^-, Al_{23}^-, and Al_{37}^- all displaying very low reactivity toward oxygen (see Fig. 12). The total valence electron numbers in these three species correspond to completed shells of 40, 70, and 112 electrons, respectively, and as such would be expected under the shell model to be particularly stable, i.e., relatively inert chemically. This is what was found. Other relevant studies include work on reactions of copper group cluster anions with both oxygen and carbon monoxide (*82*) and measurements of the dissociation energies of silver cluster anions by collision-induced dissociation (see *Thermochemistry (Methods): Collision-induced Dissociation*).

6. *Concluding Remarks*

The study of cluster anions has helped to elucidate microscopic aspects of many condensed phase phenomena and has revealed numerous unique properties not found in their corresponding bulk states. In the future, we can expect continued progress in our understanding of solvation and solid-state properties through the study of cluster anions (*83*). In particular, there is the prospect of important contributions to the materials science of electronics. This may come about in two ways. One involves contributions toward the development of cluster-assembled materials with tailored electronic (and/or magnetic) properties. The other involves the role of clusters as model systems, based on a

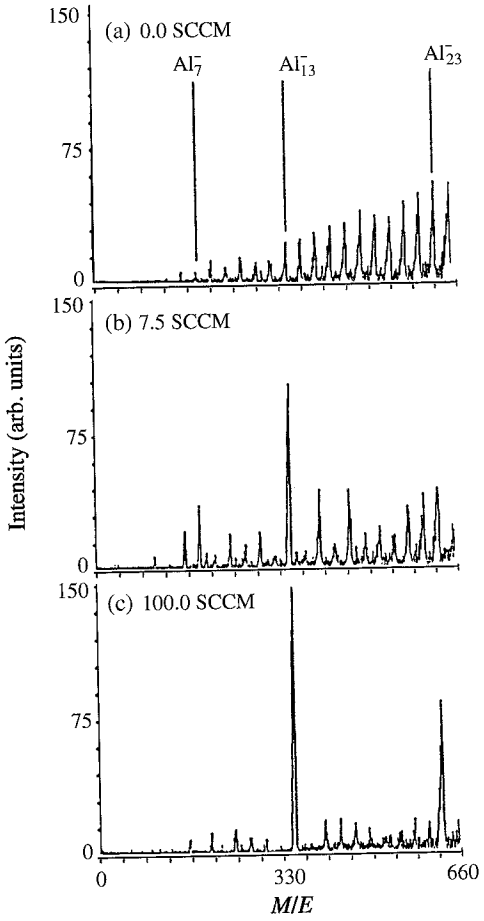

Figure 12
A series of mass spectra showing the progression of the etching reaction of aluminum cluster anions with oxygen. The flow rate is in units of sccm, standard cubic centimeters per minute. (Reproduced by permission of the American Institute of Physics from *J. Chem. Phys.* **1989**, *91*, 2753–2754 (*76*).)

recognition that the future of molecular circuits will depend on an understanding of electron attachment and transport at the microscopic level. The study of cluster anions can contribute considerably to this last frontier of electronic (and magnetic) miniaturization.

Acknowledgments

K.B. thanks The Alexander von Humboldt Foundation, NSF, DOE, and PRF for financial support as well as Sarah Stokes for her help in preparing the references and figures. E.W.S. is grateful to the Fond der Chemischen Industrie for support.

Bibliography

(*1*) Colton, R. J.; Campana, J. E.; Bariak, T. M.; DeCorpo, J. J.; Wyatt, J. R. High-performance Secondary Ion Mass Spectrometer. *Rev. Sci. Instrum.* **1980**, *51*, 1685–1689.

(*2*) Fehsenfeld, F. C.; Ferguson, E. E. Laboratory Studies of Negative Ion Reactions with Atmospheric Trace Constituents. *J. Chem. Phys.* **1974**, *61*, 3181–3193.

(*3*) Leopold, D. G.; Ho, J.; Lineberger, W. C. Photoelectron Spectroscopy of Mass-selected Metal Cluster Anions. I. Copper (Cu_n^-, $n=1$–10). *J. Chem. Phys.* **1987**, *86*, 1715–1726.

(*4*) Kaiser, H. J.; Heinicke, E.; Erhard, R.; Baumann, H.; Horst, N.; Bethge, K. Molecular and Atomic Ions of the Elements of the Subgroups A of the Periodic System. *Z. Phys.* **1971**, *243*, 46–59.

(*5*) Arshadi, M.; Yamdagni, R.; Kebarle, P. Hydration of the Halide Negative Ions in the Gas Phase. II. Comparison of Hydration Energies for the Alkali Positive and Halide Negative Ions. *J. Phys. Chem.* **1970**, *74*, 1475–1482.

(*6*) Castleman, A. W., Jr.; Tang, I. N. Heavy Metal Ion Clusters. *Nature* **1971**, *234*, 129–130.

(*7*) Moseley, J. T.; Cosby, P. C.; Bennett, R. A.; Peterson, J. R. Photodissociation and Photodetachment of Molecular Negative Ions. I. Ions Formed in Carbon Dioxide/Water Mixtures. *J. Chem. Phys.* **1975**, *62*, 4826–4834.

(*8*) Collins, J. G.; Kebarle, P. Ionization Cross-sections, Charge-transfer Cross-sections, and Ionic Fragmentation Patterns of Some Paraffins, Olefins, Acetylenes, Chloroalkanes, and Benzene with 40–100 Kev. Protons. *J. Chem. Phys.* **1967**, *46*, 1082–1089.

(*9*) Kebarle, P.; Searles, S. K.; Zolla, A.; Scarborough, J.; Arshadi, M. Solvation of the Hydrogen Ion by Water Molecules in the Gas Phase. Heats and Entropies of Solvation of Individual Reactions. $H+(H_2O)_{n-1}+H_2O \rightarrow H+(H_2O)_n$. *J. Am. Chem. Soc.* **1967**, *89*, 6393–6399.

(*10*) Moruzzi, J. L.; Phelps, A. V. Survey of Negative-ion–Molecule Reactions in Oxygen, Carbon Dioxide, Water, Carbon Monoxide, and Mixtures of these Gases at High Pressures. *J. Chem. Phys.* **1966**, *45*, 4617–4627.

(*11*) Beuhler, R. J.; Friedman, L. A Study of the Formation of High Molecular Weight Water Cluster Ions (mle < 59,000) in Expansion of Ionized Gas Mixtures. *J. Chem. Phys.* **1982**, *77*, 2549–2557.

(*12*) Siegel, M. W.; Fite, W. L. Terminal Ions in Weak Atmospheric Pressure Plasmas. Applications of Atmospheric Pressure Ionization to Trace Impurity Analysis in Gases. *J. Phys. Chem.* **1976**, *80*, 2871–2881.

(*13*) Haberland, H.; Ludewigt, C.; Schindler, H.-G.; Worsnop, D. R. Clusters of Water and Ammonia with Excess Electrons. *Surf. Sci.* **1985**, *156*, 157–164.

(*14*) Coe, J. V.; Snodgrass, J. T.; Friedhoff, C. B.; McHugh, K. M.; Bowen, K. H. Photoelectron Spectroscopy of the Negative Cluster Ions $NO^-(N_2O)_{n=1,2}$. *J. Chem. Phys.* **1987**, *87*, 4302–4309.

(*15*) Campagnola, P. J.; Posey, L. A.; Johnson, M. S. Controlling the Internal Energy Content of Size-selected Cluster Ions: An Experimental Comparison of the Metastable Decay Rate and Photofragmentation Methods of Quantifying the Internal Excitation of Hydrated Electron Clusters ($(H_2O)_n^-$). *J. Chem. Phys.* **1991**, *95*, 7998–8004.

(*16*) DesFrancois, C.; Abdoul-Carime, H.; Adjouri, C.; Khelifa, N.; Schermann, J. P. Dipole Binding to a Strongly Polar Molecule and Its Homogeneous Clusters: magic

distribution of acetonitrile cluster anions. *Europhys. Lett.* **1994**, *26*, 25–30.

(*17*) Powers, D. E.; Hansen, S. G.; Geusic, M. E.; Pulu, A. C.; Hopkins, J. B.; Dirtz, T. G.; Duncan, M. A.; Langridge-Smith, P. R. R.; Smalley, R. E. Supersonic Metal Cluster Beams: laser photoionization studies of copper cluster (Cu_2). *J. Phys. Chem.* **1982**, *86*, 2556–2560.

(*18*) Siekman, H. R.; Lueder, C.; Faehrmann, J.; Lutz, H. O.; Meiwes-Broer, K. H. The Pulsed Arc Cluster Ion Source (PACIS). *Z. Phys. D* **1991**, *20*, 417–420.

(*19*) Meng, C. K.; Fenn, J. B. Formation of Charged Clusters During Electrospray Ionization of Organic Solute Species. *Org. Mass Spectrom.* **1991**, *26*, 542–549.

(*20*) McHugh, K. M.; Sarkas, H. W.; Eaton, J. G.; Westgate, C. R.; Bowen, K. H. The Smoke Ion Source: A Device for the Generation of Cluster Ions Via Inert Gas Condensation. *Z. Phys. D.* **1989**, *12*, 3–6.

(*21*) Haberland, H.; Mall, H.; Mossler, M.; Qiang, Yi.; Reiners, T.; Thurner, Y. Filling of Micron-sized Contact Holes with Copper by Energetic Cluster Impact. *J. Vac. Sci. Technol. A.* **1994**, *12*, 2925–2930.

(*22*) Kebarle, P. Higher-order Reactions, Ion Clusters, and Ion Solvation. In *Ion–Molecule Reactions*; Franklin, J. L., Ed.; Plenum: New York, 1972, p 315.

(*23*) Keesee, R. G.; Lee, N.; Castleman, A. W., Jr. Properties of Clusters in the Gas Phase.V. Complexes of Neutral Molecules onto Negative Ions. *J. Chem. Phys.* **1980**, *73*, 2195–2202.

(*24*) Cosby, P. C.; Ling, J. H.; Peterson, J. R.; Moseley, J. T. Photodissociation and Photodetachment of Molecular Negative Ions. III. Ions Formed in Carbon Dioxide/Molecular Oxygen/Water Mixtures. *J. Chem. Phys.* **1976**, *65*, 5267–5274.

(*25*) Golub, S.; Steiner, B. Photodetachment of $[OH(H_2O)]^-$. *J. Chem. Phys.* **1968**, *49*, 5191–5192.

(*26*) Moylan, C. R.; Dodd, J. A.; Brauman, J. I. Electron Photodetachment Spectroscopy of Solvated Anions. A Probe of Structure and Energetics. *Chem. Phys. Lett.* **1985**, *118*, 38–39.

(*27*) Corderman, R. R.; Lineberger, W. C. Negative Ion Spectroscopy. *Ann. Rev. Phys. Chem.* **1979**, *30*, 347–378.

(*28*) Castleman, A. W., Jr.; Hunton, D. E.; Lindeman, T. G.; Lindsay, D. N. Studies of the Laser Photodissociation of Carbonate and Carbonate–Water Complexes. *Intl. J. Mass Spectrom. Ion Phys.* **1983**, *47*, 199–202.

(*29*) Kim, H.-S.; Bowers, M. T. Photodissociation Dynamics of Sulfur Dioxide Negative Ion Clusters: $(SO_2)_2^-$. *J. Chem. Phys.* **1986**, *85*, 2718–2725.

(*30*) Kim, J. B.; Wenthold, P. G.; Lineberger, W. C. Photoelectron Spectroscopy of $OH^-(N_2O)_{n=1-5}$. *J. Chem. Phys.* **1998**, *108*, 830–837.

(*31*) Coe, J. V.; Snodgrass, J. T.; Friedhoff, C. B.; McHugh, K. M.; Bowen, K. H. Negative Ion Photoelectron Spectroscopy of the Hydride–Ammonia Negative Cluster Ion $H^-(NH_3)_1$. *J. Chem. Phys.* **1985**, *83*, 3169–3170.

(*32*) Arnold, C. C.; Neumark, D. M.; Cyr, D. M.; Johnson, M. A. Negative Ion Zero Electron Kinetic Energy Spectroscopy of $I^-{}^{\bullet}CH_3I$. *J. Phys. Chem.* **1995**, *99*, 1633–1636.

(*33*) Ayotte, P.; Bailey, C. G.; Kim, J.; Johnson, M. A. Vibrational Predissociation Spectroscopy of the $(H_2O)_6^{-\bullet}Ar_n$, $n \geq 6$, Clusters. *J. Chem. Phys.* **1998**, *108*, 444–449.

(*34*) Bowen, K. H.; Liesegang, G. W.; Sanders, R. A.; Herschbach, D. R. Electron Attachment to Molecular Clusters by Collisional Charge Transfer. *J. Phys. Chem.* **1983**, *87*, 557–565.

(*35*) Carles, S.; Lecomte, F.; Schermann, J. P.; Desfrançois, C. Gas-phase Experimental and Theoretical Studies of Adenine, Imidazole, Pyrrole, and Water Noncovalent Complexes. *J. Phys. Chem. A* **2000**, *104*, 10662–10668.

(*36*) Albritton, D. L. Ion–Neutral Reaction-rate Constants Measured in Flow Reactors Through 1977. *At. Data Nucl. Tables.* **1978**, *22*, 1–101.

(*37*) Coe, J. V. Connecting Cluster Anion Properties to Bulk: Ion Solvation Free Energy Trends with Cluster Size and the Surface vs. Internal Nature of Iodide in Water Clusters. *J. Phys. Chem. A* **1997**, *101*, 2055–2063.

(*38*) Lee, N.; Keesee, R. G.; Castleman, A. W., Jr. The Properties of Clusters in the Gas Phase. IV. Complexes of Water and HNO_x Clustering on NO_x. *J. Chem. Phys.* **1980**, *72*, 1089–1094.

(*39*) Hendricks, J. H.; de Clercq, H. L.; Friedhoff, C. B.; Arnold, S. T.; Eaton, J. G.; Francher, C.; Lyapustina, S. A.; Snodgrass, J. T.; Bowen, K. H. Anion Solvation at the Microscopic Level: Photoelectron Spectroscopy of the Solvated Anion Clusters, $NO^-(Y)_n$, where Y = Ar, Kr, Xe, N_2O, H_2S, NH_3, H_2O, and $C_2H(OH)_2$. *J. Chem. Phys.* **2002**, *116*, 7926–7938.

(*40*) Schiedt, J.; Knott, W. J.; Le Barbu, K.; Schlag, E. W. Microsolvation of Similar-sized Aromatic Molecules: Photoelectron Spectroscopy of Bithiophene$^-$, Azulene$^-$, and Naphthalene–Water Anion Clusters. *J. Chem. Phys.* **2000**, *113*, 9470–9478.

(*41*) Le Barbu, K.; Schiedt, J.; Weinkauf, R.; Schlag, E. W.; Nilles, J. M.; Xu, S.-J.; Thomas, O. C.; Bowen, K. H. Microsolvation of Small Anions by Aromatic Molecules: An Exploratory Study. *J. Chem. Phys.* **2002**, *116*, 9663–9671.

(*42*) Arnold, D. W.; Bradforth, S. E.; Kim, E.; Neumark, D. M. Study of $I^-(CO_2)_n$, $Br^-(CO_2)_n$, and $I^-(N_2O)_n$ Clusters by Anion Photoelectron Spectroscopy. *J. Chem. Phys.* **1995**, *102*, 3510–3518.

(*43*) Wang, X.-B.; Yang, X.; Wang, L.-S. Photodetachment and Theoretical Study of Free and Water-solvated Nitrate Anions, $NO_3^-(H_2O)_n$ ($n = 0-6$). *J. Chem. Phys.* **2002**, *116*, 561–570.

(*44*) Arnold, S. T.; Hendricks, J. H.; Bowen, K. H. Photoelectron Spectroscopy of the Solvated Anion Clusters $O^-(Ar)_{n=1-26,34}$: Energetics and Structure. *J. Chem. Phys.* **1995**, *102*, 39–47.

(*45*) Müller-Dethlefs, K.; Schlag, E. W. High-resolution Zero Electron Kinetic Energy (ZEKE) Photoelectron Spectroscopy of Molecular Systems. *Annu. Rev. Phys. Chem.* **1991**, *42*, 109–136.

(*46*) Alexander, M. L.; Levinger, N. E.; Ray, D. R.; Johnson, M. A.; Lineberger, W. C. Recombination of Bromine Diatomic Mononegative Ion Photodissociated within Mass-selected Ionic Clusters. *J. Chem. Phys.* **1988**, *88*, 6200–6210.

(*47*) Greenblatt, B. J.; Zanni, M. T.; Neumark, D. M. Femtosecond Photoelectron Spectroscopy of $I_2^-(CO_2)_n$ Clusters ($n = 4,6,9,12,14,16$). *J. Chem. Phys.* **2000**, *112*, 601–612.

(*48*) Davis, A. V.; Wester, R.; Bragg, A. E.; Neumark, D. M. Vibrational Relaxation in Clusters: Energy Transfer in $I_2^-(CO_2)_4$ Excited by Femtosecond Stimulated Emission Pumping. *J. Chem. Phys.* **2002**, *117*, 4282–4292.

(*49*) Cyr, D. M.; Bishea, G. A.; Scarton, M. G.; Johnson, M. A. Observation of Charge-transfer Excited States in the Iodide–Iodomethane, Iodide–Bromomethane, and Iodide–Dibromomethane (I^-–CH_3I,I^-–CH_3Br, and

$I^-CH_2Br_2$) S_N2 Reaction Intermediates Using Photofragmentation and Photoelectronic Spectroscopies. *J. Chem. Phys.* **1992**, *97*, 5911–5914.
(*50*) Clements, T. G.; Luong, A. K.; Deyeri, H.-J.; Continetti, R. E. Dissociative Photodetachment Studies of $O^-(H_2O)_2$, $OH^-(H_2O)_2$, and the Deuterated Isotopomers: Energetics and Three-Body Dissociation Dynamics. *J. Chem. Phys.* **2001**, *114*, 8436–8444.
(*51*) Ayotte, P.; Nielsen, S. B.; Weddle, G. H.; Johnson, M. A.; Xantheas, S. S. Spectroscopic Observation of Ion-induced Water Dimer Dissociation in the $X^{-\bullet}(H_2O)_2$ (X = F, Cl, Br, I) Clusters. *J. Phys. Chem. A* **1999**, *103*, 10665–10669.
(*52*) Cabarcos, O. M.; Weinheimer, C. J.; Lisy, J. M.; Xantheas, S. S. Microscopic Hydration of the Fluoride Anion. *J. Chem. Phys.* **1999**, *110*, 5–8.
(*53*) Okumura, M.; Choi, J. H.; Kuwata, K. T.; Cao, Y. B.; Haas, B. M. Infrared Spectroscopy of Hydrated Halide Ion Clusters. *SPIE Proc.* **1995**, *2548*, 147–156.
(*54*) Serxner, D.; Dessent, C. E. H.; Johnson, M. A. Precursor of the I^-_{aq} Charge-transfer-to-solvent (CTTS Band). *J. Chem. Phys.* **1996**, *105*, 7231–7234.
(*55*) Yang, X.; Zhang, X.; Castleman, A. W., Jr. Chemistry of Large Hydrated Anion Clusters $X^-(H_2O)_n$, $n = 0$–59 and X = OH, O, O_2, and O_3. 2. Reaction of CH_3CN. *J. Phys. Chem.* **1991**, *95*, 8520–8524.
(*56*) Yang, X.; Castleman, A. W., Jr. Chemistry of Large Hydrated Anion Clusters $X^-(H_2O)_n$, $n = 0$–59 and X = OH, O, O_2 and O_3. 3. Reaction of SO_2. *J. Phys. Chem.* **1991**, *95*, 6182–6186.
(*57*) Yasumatsu, H.; Terasakia, A.; Kondow, T. Charge Transfer from I_2^--$(CO_2)_n$ Cluster Anion to Silicon Surface: Cluster-Size Dependence. *Int. J. Mass Spectrom.* **1998**, *174*, 297–303.
(*58*) Armbruster, M.; Haberland, H.; Schindler, H.-G. Negatively Charged Water Clusters, or the First Observation of Free Hydrated Electrons. *Phys. Rev. Lett.* **1981**, *47*, 323–326.
(*59*) Klots, C. E.; Compton, R. N. Electron Attachment to Carbon Dioxide Clusters in a Beam. *J. Chem. Phys.* **1977**, *64*, 1779–1780.
(*60*) Wang, X.; Wang, X. B.; Wang, L.-S. Photodetachment of Hydrated Sulfate Doubly Charged Anions: $SO_4^{2-}(H_2O)_n$ ($n = 4$–40). *J. Phys. Chem. A* **2002**, *106*, 7607–7616.
(*61*) Thomas, O. C.; Zheng, W.-J.; Xu, S.-J.; Bowen, K. H. Onset of Metallic Behavior in Magnesium Clusters. *Phys. Rev. Lett.* **2002**, *89*, 213403/1–213403/4.
(*62*) Mitsui, M.; Nakajima, A.; Kaya, K.; Even, U. Mass Spectra and Photoelectron Spectroscopy of Negatively Charged Benzene Clusters, $(Benzene)_n^-$ ($n = 53$–124). *J. Chem. Phys.* **2001**, *115*, 5707–5710.
(*63*) Coe, J. V.; Lee, G. H.; Eaton, J. G.; Arnold, S. T.; Sarkas, H.; Bowen, K. H.; Ludewigt, C.; Haberland, H.; Worsnop, D. R. Photoelectron Spectroscopy of Hydrated Electron Cluster Anions $(H_2O)^-_{n=2-69}$. *J. Chem. Phys.* **1990**, *92*, 3980–3982.
(*64*) Kim, J.; Becker, I.; Cheshnovsky, O.; Johnson, M. A. Photoelectron Spectroscopy of the 'Missing' Hydrated Electron Clusters $(H_2O)_n^-$, $n = 3$, 5, 8, and 9: Isomers and Continuity with the Dominant Clusters $n = 6$, 7 and ≥ 11. *Chem. Phys. Lett.* **1998**, *297*, 90–96.
(*65*) Sarkas, H. W.; Arnold, S. T.; Eaton, J. G.; Lee, G. H.; Bowen, K. H. Ammonia Cluster Anions and their Relationship to Ammoniated (Solvated) Electrons: The Photoelectron Spectra of $(NH_3)^-_{n=41-1,100}$. *J. Chem. Phys.* **2002**, *116*, 5731–5737.
(*66*) Takasu, R.; Ito, H.; Nishikawa, K.; Hashimoto, K.; Okuda, R.; Fuke, K. Solvation Process of Na_m in Small Ammonia Clusters: Photoelectron Spectroscopy of $Na_m^-(NH_3)_n$ ($m \leq 3$). *J. Elec. Spec.* **2000**, *106*, 127–139.
(*67*) Lehr, L.; Zanni, M. T.; Frischkorn, C.; Weinkauf, R.; Neumark, D. M. Electron Solvation In Finite Systems: Femtosecond Dynamics of Iodide–$(Water)_n$Anion Clusters. *Science* **1999**, *284*, 635–638.
(*68*) Hendricks, J. H.; de Clercq, H. L.; Lyapustina, S. A.; Bowen, K. H. Negative Ion Photoelectron Spectroscopy of the Ground State, Dipole-bound Dimeric Anion $(HF)_2^-$. *J. Chem. Phys.* **1997**, *107*, 2962–2967.
(*69*) Gutowski, M.; Hall-Black, C. S.; Adamowicz, L.; Hendricks, J. H.; de Clercq, H. L.; Lyapustina, S. A.; Nilles, J. M.; Xu, S.-J.; Bowen, K. H., Jr. Solvated Electrons in Very Small Clusters of Polar Molecules: $(HF)_3^-$. *Phys. Rev. Lett.* **2002**, *88*, 143001/1–143001/4.
(*70*) Lyapustina, S. A.; Xu, S.-J.; Nilles, J. M.; Bowen, K. H., Jr. Solvent-induced Stabilization of the Naphthalene Anion by Water Molecules: A Negative Cluster Ion Photoelectron Spectroscopic Study. *J. Chem. Phys.* **2000**, *112*, 6643–6648.
(*71*) Yang, Y. A.; Bloomfield, L. A.; Jin, C.; Wang, L.-S.; Smalley, R. E. Ultraviolet Photoelectron Spectroscopy and Photofragmentation Studies of Excess Electrons in Potassium Iodide Cluster Anions. *J. Chem. Phys.* **1992**, *96*, 2453–2459.
(*72*) Campagnola, P. J.; Lavrich, D. J.; DeLuca, M. J.; Johnson, M. A. Photodestruction Spectra of the Anionic Water Clusters, $(H_2O)_n^-$, $n = 18$ and 30: Absorption to the Red of Hydrated Electron (e^-_{aq}). *J. Chem. Phys.* **1991**, *94*, 5240–5242.
(*73*) Arnold, S. T.; Morris, R. A.; Viggiano, A. A.; Johnson, M. A. Thermal Energy Reactions of Size-selected Hydrated Electron Clusters $(H_2O)_n^-$. *J. Phys. Chem.* **1996**, *100*, 2900–2906.
(*74*) Kondow, T. Ionization of Clusters in Collision with High-Rydberg Rare Gas Atoms. *J. Phys. Chem.* **1987**, *91*, 1307–1316.
(*75*) Cohen, M. L.; Knight, W. D. The Physics of Metal Clusters. *Physics Today* **1990**, *December*, 42–50.
(*76*) Leuchtner, R. E.; Harms, A. C.; Castleman, A. W., Jr. Thermal Metal Cluster Anion Reactions: Behavior of Aluminum Clusters with Oxygen. *J. Chem. Phys.* **1989**, *91*, 2753–2754.
(*77*) Ho, J.; Ervin, K. M.; Lineberger, W. C. Photoelectron Spectroscopy of Metal Cluster Anions:Cu_n^-, Ag_n^-, and Au_n^-. *J. Chem. Phys.* **1990**, *93*, 6987–7002.
(*78*) Cheshnovsky, O.; Taylor, K. J.; Conceicao, J.; Smalley, R. E. Ultraviolet Photoelectron Spectra of Mass-selected Copper Clusters: Evolution of the 3d Band. *Phys. Rev. Lett.* **1990**, *64*, 1785–1788.
(*79*) Cha, C-Y.; Ganteför, G.; Eberhardt, W. Photoelectron Spectroscopy of Copper Mononegative Ion (Cu_n^-) Clusters: Comparison with Jellium Model Predictions. *J. Chem. Phys.* **1993**, *99*, 6308–6312.
(*80*) Li, X.; Wu, H.; Wang, X.-B.; Wang, L.-S. s–p Hybridization and Electron Shell Structures in Aluminum Clusters: A Photoelectron Spectroscopy Study. *Phys. Rev. Lett.* **1998**, *81*, 1909–1912.
(*81*) Eaton, J. G.; Kidder, L. H.; Sarkas, H. W.; Bowen, K. H. Photoelectron Spectroscopy of Alkali Metal Cluster Anions. In *Lecture Notes in Physics 404 (Nucl. Phys. Concepts Study At. Cluster Phys.)*; Schmidt, R., Lutz, H. O., Dreizler, R., Eds.; Springer-Verlag: Berlin, 1992, p 291.

(82) Lee, T. H.; Ervin, K. M. Reactions of Copper Group Cluster Anions with Oxygen and Carbon Monoxide. *J. Phys. Chem.* **1994**, *98*, 10023–10031.
(83) Castleman, A. W., Jr.; Bowen, K. H. Clusters: Structure, Energetics, and Dynamics of Intermediate States of Matter. *J. Phys. Chem.* **1996**, *100*, 12911–12944.

K. H. Bowen Jr.
Johns Hopkins University, Baltimore, Maryland, USA

E. W. Schlag
Technische Universität Munich, Garching, Germany

Metal Ion Solvation

1. Introduction

The question: How to study solvation in the gas phase where you have no solvent? Answer: Start small and build the solvation sphere one solvent molecule at a time. In the process, gas-phase studies of solvation can provide quantitative insight into solvation phenomena. In this article, the focus is on solvation of metal ions, a topic that has seen extensive growth over the last decade. Solvated metal ions are of general interest in solvation phenomena, but are also important in chemical and biological disciplines as a result of their scientific importance and potential technological applications.

The data in Table 1 show whether such an extrapolation is reasonable for the case of hydration of singly charged alkali ions and doubly charged alkaline earth ions. In the gas phase, the sequential hydration enthalpies are determined for reaction (1).

$$M^{n+}(H_2O)_x \rightarrow M^{n+}(H_2O)_{x-1} + H_2O \qquad (1)$$

In the case of the alkali ions, it can be seen that the sum of the first six enthalpy changes (approximately one complete solvent shell) reproduces the bulk-phase hydration enthalpy. Although this absolute agreement is serendipitous, the fact that the relative values for the clusters agree with the relative hydration energies means that all metal specific interactions are included in this first solvent shell. Agreement for the doubly charged group 2 ions is not as favorable even though 14 water molecules are included. Presumably the higher charge density of these ions influences the binding of additional solvent molecules well beyond the first solvent shell. Note however that the relative value, the difference between the values for Mg^{2+} and Ca^{2+}, is reproduced: 338 kJ mol^{-1} from the gas-phase data and 329 kJ mol^{-1} from the solution-phase results. Thus the inner solvent shell again appears to contain all the metal specific information in the hydration enthalpies. Similar observations have been made for other types of ions (see *Solvation and Clusters: The Ionic Hydrogen Bond in Complex Organics and Biomolecules*).

Table 1
Comparison between gas-phase hydration enthalpy sums and solution-phase hydration enthalpies for singly and double charged metal ions (all values in kJ mol^{-1}).

Cation	Max x	$\Sigma\Delta H_{x,x-1}$ [a]	$\Delta H_{hydration}$ [b]
Li^+	6	-539 ± 19 [c]	−515
Na^+	6	-406 ± 20 [d]	−406
K^+	6	-330 ± 20 [d]	−321
Mg^{2+}	14	-1819 ± 31 [e]	−1952
Ca^{2+}	14	-1481 ± 31 [e]	−1623

[a] Sum of individual hydration enthalpies from $x = 1$ to max x. [b] Ref (*1*) referenced to a value of −1091 kJ mol^{-1} for the proton (*2*). See also (*3*), who determine $\Delta H_{hydration}(H^+) = -1150$ kJ mol^{-1}. [c] Ref (*4*). [d] Ref (*5*). [e] Ref (*6*).

2. Trends in Stabilities and Structures in the Solvation of Different Metal Monocations

To illustrate the trends that can occur as different metal ions are solvated, we focus on ammonia. NH_3 is capable of hydrogen bonding, although the propensity for this is not as great as that of H_2O, but more than most other ligands. It has the simplifying feature that it is largely a sigma donor in which the lone pair of electrons on the nitrogen donates into orbitals on the metal ion. Interaction in the π space is limited, unlike water, which is a weak π donor, or carbon monoxide, which is a strong π acceptor. Further there is extensive data for solvation of many different ions by ammonia, although not yet quite as complete a database as for water. (For more complete thermodynamic information on these and other ligands bound to metal ions, see references (*7–9*) as well as *Thermochemistry (Methods): Thermochemistry Definitions and Tabulations.*) Such data have been acquired largely by using both high-pressure equilibrium methods (see *Thermochemistry (Methods): Ion–Molecule Equilibria at High Pressure*) and collision-induced dissociation experiments (see *Thermochemistry (Methods): Collision-induced Dissociation*). Although data for ammonia are presented here to illustrate the various trends, water is arguably the most important solvent and the interested reader is referred to reference (*7*) for a similar discussion of the specific interactions of metal ions with varying numbers of water molecules, including the analogue to Fig. 1.

Figure 1 shows the bond energies between ammonia and several types of singly charged metal ions: the alkalis (Li^+–Rb^+) (*4*, *8*, *10–14*), an alkaline earth (Mg^+) (*15*), the first row transition metals (Ti^+–Cu^+) (*16*), a third row transition metal (Pt^+) (*17*), and a heavy main group metal (Pb^+) (*18*). Clearly the